Easy Cleaning of 3D SLA/DLP Printed Soft Fluidic Actuators with Complex Internal Geometry

Benn W.B. Proper[1*], Brandon J. Caasenbrood[1], and Irene A. Kuling[1]

***Abstract*— With the rise of new applications for soft actuators, more advanced methods of fabrication are being used to obtain the desired complex internal structures. Due to their accuracy, affordability, and ability to create airtight structures, Stereolithography (SLA) and Digital Light Processing (DLP) printing are becoming increasingly common for manufacturing these soft fluidic actuators (SFAs). The manufacturing of SFAs using these printing methods requires various post-processing steps to ensure that the final result exhibits the desired behavior when pressurized. However, the required steps are often poorly documented and mainly focus on cleaning the exterior of an SLA/DLP printed part. In this paper, we provide a methodology to clean the complex internal structures of SLA/DLP printed SFAs. This methodology comes in the form of a peristaltic pump used to cycle the cleaning liquid through the internal geometry of the SFA, and a clear cleaning procedure. We compare our cleaning procedure to the standard procedure, showing the effectiveness of the proposed method.**

I. Introduction

The field of soft robotics is a rapidly growing field where primarily soft materials with properties similar to soft biological materials are used to create continuum robots [1], [2], [3]. These systems are used for a variety of purposes such as minimally invasive surgery [4], wearable for rehabilitation [5], and grippers [6]. Although there are many different types of actuation [7], Soft Fluidic Actuators (SFAs) [8] are frequently used because of their adaptive capabilities with respect to surrounding objects [3], [9]. SFAs typically have internal cavities to obtain the desired movement action and to make these geometries, uncured silicon rubber is poured into molds [10]. Given the recent advances in additive manufacturing, especially with highly-flexible materials, 3D printing is being used to manufacture soft actuators [11], [12]. Fused Deposition Modeling (FDM), Stereolithography (SLA), and Digital Light Processing (DLP) are common 3D printing techniques. While FDM is accessible and is a low-cost option [13], to avoid air leakage, over-extrusion is needed [14], which limits the accuracy of printing. SLA and DLP printers, while being more expensive, are more accurate and can even achieve sub-micrometer resolution [15], and are less susceptible to air leakage. Focusing on SLA and DLP printers, these techniques use UV light to pattern an object layer-by-layer using a photocuring liquid resin. When SFAs are produced through SLA or DLP, the uncured resin will collect in various recesses, requiring a cleanup step before performing the post-curing step to achieve the highest possible strength and stability. Without sufficient cleanup, the excess resin will cure during the post-curing step and will compromise the desired internal geometry of the SFA as shown in Fig. 1.

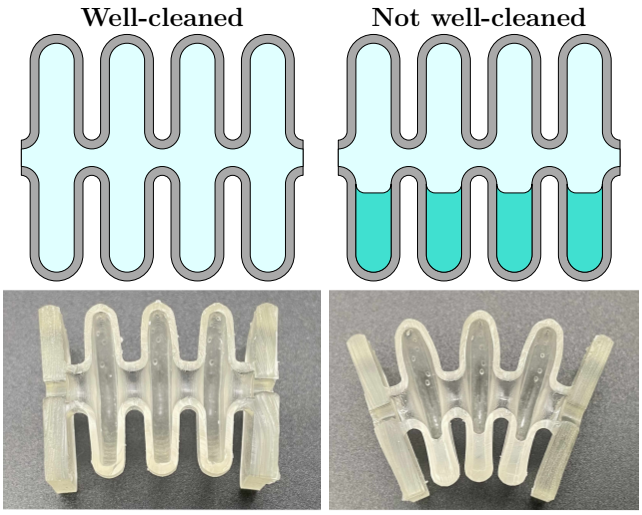

Fig. 1: Examples of the cleaned and uncleaned insides of a single-bellow SFA. The top and bottom rows show schematic and real illustrations of the longitudinal section of the SFA, respectively. In the schematics, grey is the wall of the SFA, light blue is the inside of the SFA, and greenish blue is excess cured resin due to insufficient cleaning before post-curing. For the bottom row, the excess cured resin shows as a solid mass of resin connecting two walls of the SFA, resulting in undesired deformation of the actuator.

The cleaning procedure for SLA/DLP printed SFAs is often poorly documented, for example, either the cleaning procedure is skipped over to discuss the post-curing step [16] or it is mentioned without specifications on the used methods [17]. In some cases, cleaning procedures that deviate from the recommended cleaning steps are presented, where specialized equipment is used to clean the SFAs [15], [18]. However, in a majority of academic work, the cleaning and post-curing steps are not discussed at all [19], [20], [21], [22]. This non-specificity of the cleaning procedures and in some cases the use of specialized non-standard cleaning equipment complicates the reproducibility of these works. Additionally, the lack of detailed cleaning procedures to clean internal geometries in SLA/DLP printed parts makes it difficult to reliably manufacture SFAs that perform as desired.

This paper proposes a methodology for the cleaning step of manufacturing SLA/DLP printed SFAs. We focus on cleaning SLA printed SFAs, but due to the similarities between SLA and DLP printing, the proposed procedure is also applicable to DLP printed parts. The cleaning procedure is supported by an easy-to-manufacture peristaltic pump. The

[1] Department of Mechanical Engineering, Eindhoven University of Technology (TU/e), 5600MB Eindhoven, The Netherlands.
* Corresponding author. Email: b.w.b.proper@tue.nl

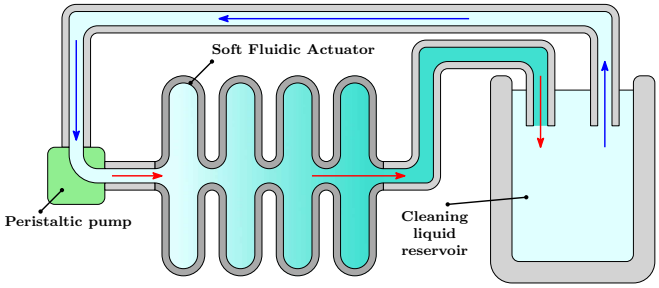

Fig. 2: Diagram of the proposed cleaning procedure. A peristaltic pump pumps a cleaning liquid through the SFA, removing internal uncured resin.

proposed procedure is shown in Fig. 2, where the peristaltic pump will pump a cleaning liquid through the SFA, removing any uncured resin. To highlight the importance of the crucial step of post-processing, we compare the SFAs cleaned with our procedure with the cleaning procedure typically recommended for SLA/DLP printed parts. The manufacturing of the pump is discussed in Sec. II. Afterward, the printing and cleaning procedure is discussed in Sec. III. Finally, in Sec. IV, three-bellow SFAs are cleaned using the standard and the proposed procedure, showing the effectiveness of our proposed method.

II. Peristaltic Pump Construction

The components of the peristaltic pump used to clean the internal structure of SLA/DLP printed SFAs can be separated into three sets of components. Namely, the assembly that allows for the pumping motion when actuated (II-A), the electronic components required to control the flow (II-B), and additional recommended components II-C.

A. Peristaltic Pump Assembly

To facilitate ease of manufacturing, most of the components of the assembly are 3D printed and the overall design of the assembly is an iteration on an open-source design for a peristaltic pump for use with a NEMA 17 stepper motor [23]. This design was iterated under the Creative Commons Attribution-NonCommercial 4.0 International license. The original design allowed for one motor to induce fluid flow in one channel of $6\,\mathrm{x}4\,\mathrm{mm}$ soft silicon tubing.

To allow for one motor to induce fluid flow in multiple channels, the original design was iterated to include flanges on the base and top of an individual channel assembly, allowing for connecting individual channel assemblies in series. To allow a single motor to pump all channels, a connecting piece was designed that connects individual bearing holders. On one end, the connecting piece is stuck with a friction fit, while the other side has a loose fit which reduces the chance of the pump jamming when multiple segments are connected in series. The merit advantage of using one motor to power multiple channels is the reduction of the complexity and costs of the electronic components. The modular design allows for a simple method to get the required number of channels for each cleaning project. The pump assembly with three channels is shown in Fig. 3. The 3D-printed components were printed using FDM with Polylactic Acid (PLA) and the

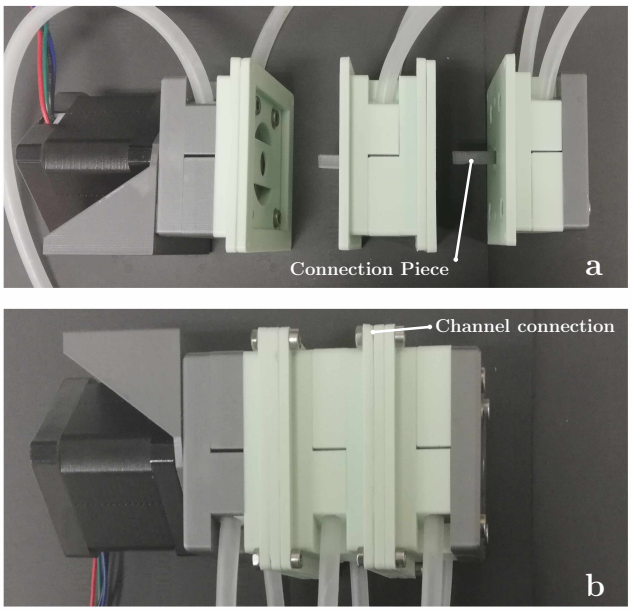

Fig. 3: Constructed pump assembly with three channels attached to the stepper motor. (a) The three individual separated channels are shown. (b) The fully assembled pump is shown from the side, where individual channels are connected at the flanges and the connecting piece ensures all bearing holders rotate in unison.

models and off-the-shelf components necessary to assemble a channel assembly can be found in [24].

B. Flow Regulation

To actuate the pump assembly, the stepper motor needs to be connected to the necessary electronics. The main components that are required for the pump to function are the control board, the stepper motor, the motor driver module, and the power supply. For this pump, we also use a potentiometer to allow for controlling the speed of the stepper motor.

For the control board, we use an Arduino Uno, that acts as a speed regulator to the stepper motor using an analog input from a potentiometer. As stated in Sec. II-A, the stepper motor that is used is a NEMA 17 stepper motor which has sufficient power to pump at least three fluid channels at once with a single motor. To support controlling the stepper motor, an A4988 motor driver module is used, as this was affordable and available while being sufficient for our purpose. Finally, both the Arduino and the stepper motor are powered by a single $12\,\mathrm{V}$ and $2\,\mathrm{A}$ power supply. The Arduino code, connection diagram, and electronic components list for this setup can be found in [24].

C. Additional Components

Additional components are required to ensure satisfactory performance of the pump for the cleaning process; an attachment plate to connect the SFA to the peristaltic pump, and an anchor to weigh down the fluid intake. The attachment plate is designed with two nozzles on either side of the plate, one designed to fit on the SFA, and the other designed to attach to the silicon tubing using the elasticity of the tubing and friction. The plate is attached to the SFA by screwing the

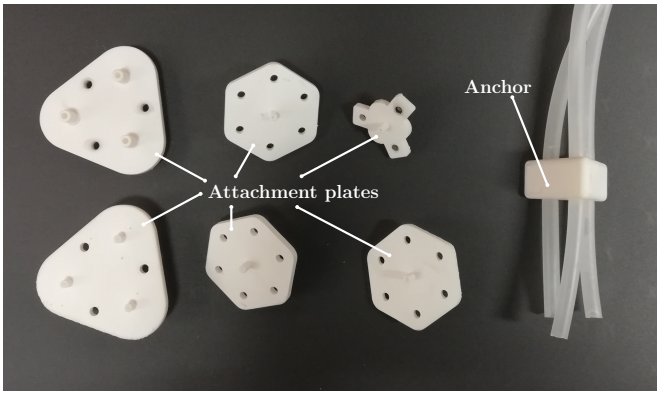

Fig. 4: Several examples of attachment plates to attach the peristaltic pump to the to-be-cleaned SFAs and hose anchors to ensure that the fluid intake remains mostly stationary. These parts were 3D-printed on a Formlabs Form 3+ SLA printer with Rigid 10k hard resin to provide sufficient weight to weigh down the tubing to ensure it remains inside the liquid.

two parts together. Without proper screw attachment, these parts can easily disconnect since the submerged fluid of resin and used cleaning liquid acts like a lubricant.

The anchor is designed for the silicon tubing to be threaded through and to ensure that the fluid intake remains inside the liquid. Without an anchor, the peristaltic pump will induce vibrations into the silicon tubing. This introduces the risk of the fluid intake leaving the cleaning liquid and pumping air instead. Several examples of attachment plates as well as an anchor are shown in Fig. 4.

III. Manufacturing and Cleaning SFAs

This section discusses the used 3D printer setup and settings (III-A), the standard cleaning procedure (III-B), and the proposed cleaning procedure using the peristaltic pump described in the previous section (III-C).

A. Printing Setup

The SFAs are printed with a Formlabs Form 3+ SLA printer using Flexible 80A soft resin with a $1\,\mathrm{micron}$ layer height. Supports are automatically generated using the Rigid 10k support settings with internal supports turned off. These settings result in a more sparse support placement, reducing support cleanup after printing, while still being quick to generate. Additional supports are added to the model in places where it is deemed necessary.

To clean the outside of the SFAs after printing, the Form Wash is used and is filled with Tripropylene Glycol Monomethyl ether (TPM). To ensure that fluid flow can be established throughout the SFA, the SFA is printed with holes on both ends. One of the holes can be sealed during post-processing to allow for pressurization.

B. Standard Cleaning Procedure

To provide a basis for our cleaning procedure to be built upon, the standard cleaning procedure recommended by Formlabs is used [25]. In short, these steps are:

1) Pre-rinse internal channels with ethanol.
2) Place SFA in reservoir of TPM or Isopropyl Alcohol (IPA).
3) Agitate the liquid for the recommended wash time for the used material ($20\,\mathrm{min}$ of total wash time, rinsing the part with water halfway for Flexible 80A).
4) Remove SFA from the reservoir and rinse with water.
5) Once the SFA is fully dry, perform the post-curing step of the SFA according to the specifications of the used material ($10\,\mathrm{min}$ at $70\,^{\circ}\mathrm{C}$ for Flexible 80A).

C. Cleaning Procedure with Pump

Our cleaning procedure expands on the original cleaning procedure by adding a peristaltic pump to cycle the cleaning liquid through the SFA. Our procedure consists of several additional steps but requires little active involvement with the process. The step-by-step cleaning process using our pump is as follows:

1) Screw attachment plate to the SFA and attach the pumping channels to the attachment plate (Fig. 5 b).
2) Drop the fluid intake and SFA into a reservoir filled with TPM and activate the pump (Fig. 5 c).
3) To ensure that the TPM covers the most surface area, agitate the SFA to remove any excess air.
4) Pump TPM through the SFA for at least 2 hours. Longer pumping times result in better cleaning results.
5) To ensure that TPM touches the entire inside, regardless of potential trapped air, rotate the SFA every 30 minutes.
6) Remove SFA from the TPM reservoir and drain liquid.
7) Move SFA and intake to reservoir of water (Fig. 5 d).
8) Rinse excess leftover TPM from the SFA with water.
9) Replace water with clean water.
10) Repeat step 2, 3, 4, and 5 with water instead of TPM for at least 1 hour.
11) Remove the SFA from the water reservoir, disconnect the pump, and drain the water.
12) Once the SFA is fully dry, perform the post-curing step of the SFA according to the specifications of the used material ($10\,\mathrm{min}$ at $70\,^{\circ}\mathrm{C}$ for Flexible 80A).

If there is still some residual resin inside the SFA, repeat the cleaning procedure from the start until the results are satisfactory. For the post-curing step, we cure the printer part at the time and temperature mentioned in the Flexible 80A datasheet, which is $10\,\mathrm{min}$ at $70\,^{\circ}\mathrm{C}$. Besides the recommendation of using TPM to clean the SLA printed part, other options for the printing, washing, and post-curing equipment can be used as the cleaning procedure discussed in Sec. III-C does not rely on Formlabs equipment. As was stated prior, the SFAs cleaned using this method need an opening on both ends to facilitate fluid flow. To seal one side of the SFA to allow for pressurization, a plug is designed based on the geometry of the holes. This plug is covered with uncured resin and plugged into one end of the SFA. Using the post-curing chamber, the plugged SFA is sealed completely as the uncured resin will fill all possible air gaps. The process of plugging these holes is shown in Fig. 6

Before cleaning the SLA/DLP printed SFA, an important consideration for the cleaning liquid needs to be taken into

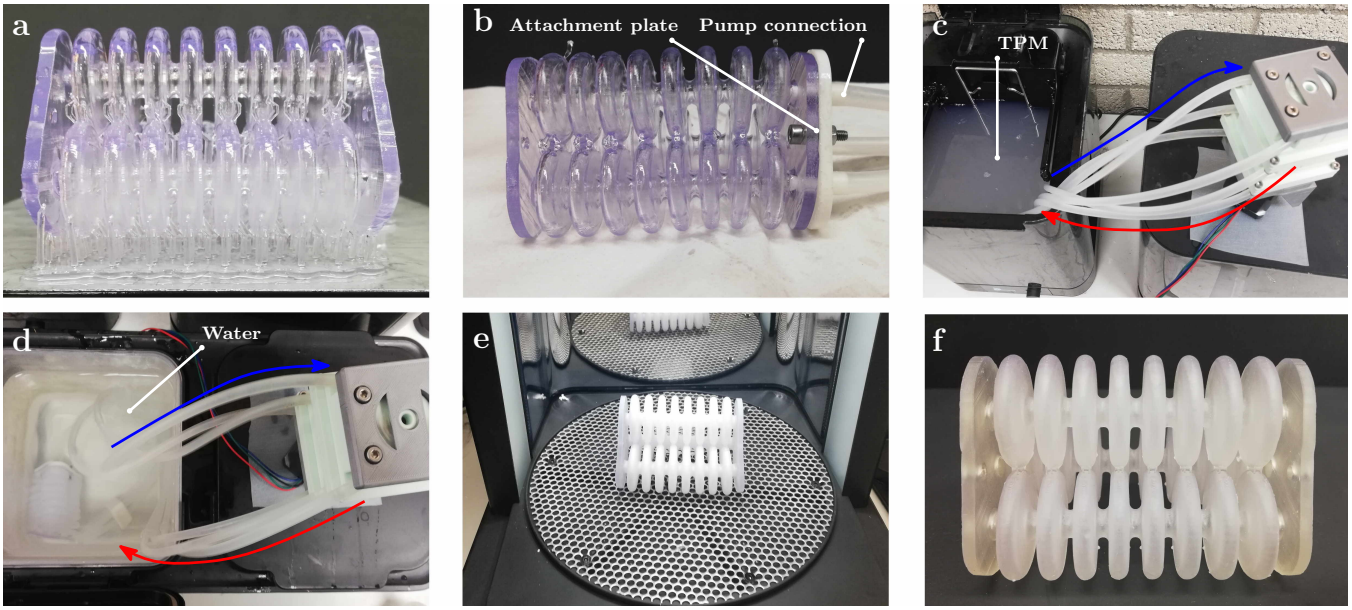

Fig. 5: Example of cleaning procedure applied to a three-bellow SFA. (a) The SFA on the printbed. (b) The SFA attached to the pump. (c) TPM is circulated through the SFA while placed in the TPM reservoir. (d) The SFA is placed in the water reservoir to rinse out excess TPM. (e) The SFA is placed in the post-curing chamber. (f) The fully cured three-bellow SFA.

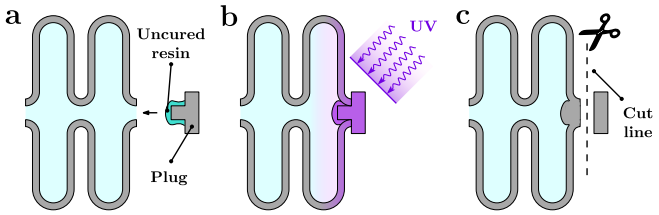

Fig. 6: Sealing procedure for SLA/DLP printed SFAs. (a) A plug is covered in uncured resin and inserted in one end of the SFA. (b) The plugged SFA is cured using UV light. (c) The top of the plug is cut off to ensure that there is no excess material on the end of an SFA.

account. For our cleaning procedure, the SFA will remain in the cleaning liquid reservoir for at least two hours. If IPA is used as a cleaning liquid, there is a significant risk of warping of the print if left in prolonged contact. For this reason, as well as the low volatility, TPM being non-flammable, and it being non-toxic, we prefer using TPM as a cleaning liquid.

IV. Cleaning Procedure Assessment

This section assesses the effectiveness of our cleaning procedure by printing and cleaning several SFAs. The methods of obtaining the control group of SFAs and SFAs cleaned with our procedure are discussed in Sec. IV-A. This is followed by comparing the motion when pressurizing the chambers for the control group and the three-bellow SFAs cleaned with our procedure in Sec. IV-B. Testing the functionality of SFAs was done using the Soft Robotics Control-unit (SRC) [26].

A. Methods of Manufacturing SFAs

To compare our cleaning procedure to the standard cleaning procedure, the Eindhoven University of Technology (TU/e) 3D printer service [27] was used to obtain a control group of SFAs. This printer service uses the recommended cleaning procedure described by Formlabs described in Sec. III-C. Furthermore, this printer service provides the option to clean SLA/DLP printed parts with either TPM or IPA and allows for an optional pre-rinse with ethanol to clean out the internal geometry. To assess whether the cleaning liquid and pre-rinsing have a significant effect on the quality of printing SFAs using the standard procedure, four three-bellow SFAs were requested. Two of the requested SFAs were pre-rinsed with ethanol, while the remaining two were not. Of the pre-rinsed SFAs, one was cleaned in a reservoir of TPM and the other in IPA, likewise for the non-pre-rinsed SFAs.

Four three-bellow SFAs were printed and cleaned using our method described in Sec. III-C. Additionally, to assess whether the cleaning procedure works regardless of the type of SFA cleaned, three additional SFA types were printed and cleaned. These include a soft gripper that closes when a positive pressure difference is applied, a topology-optimized bending actuator, and a topology-optimized soft gripper that uses both compliant mechanisms and a vacuum bellow to grip objects [28], [29]. Finally, all SFAs are plugged according to the method described in Fig. 6.

B. Cleaning Procedure Comparison

The three-bellow bending actuator is designed with three connected bellows that have separate air chambers. By pressurizing one or multiple bellows, the actuator can move one end relative to the other in 3 dimensions. The internal structure of this SFA consists of three separate channels and many narrow areas, where fluid flow is difficult, resulting in many possibilities of resin buildup.

To compare the control group with our sample group, all three-bellow SFAs are subjected to the same pressure reference. The pressure reference is given by:

$$u_i(t) = P_0 + P_a \sin(\omega t + \phi_i), \tag{1}$$

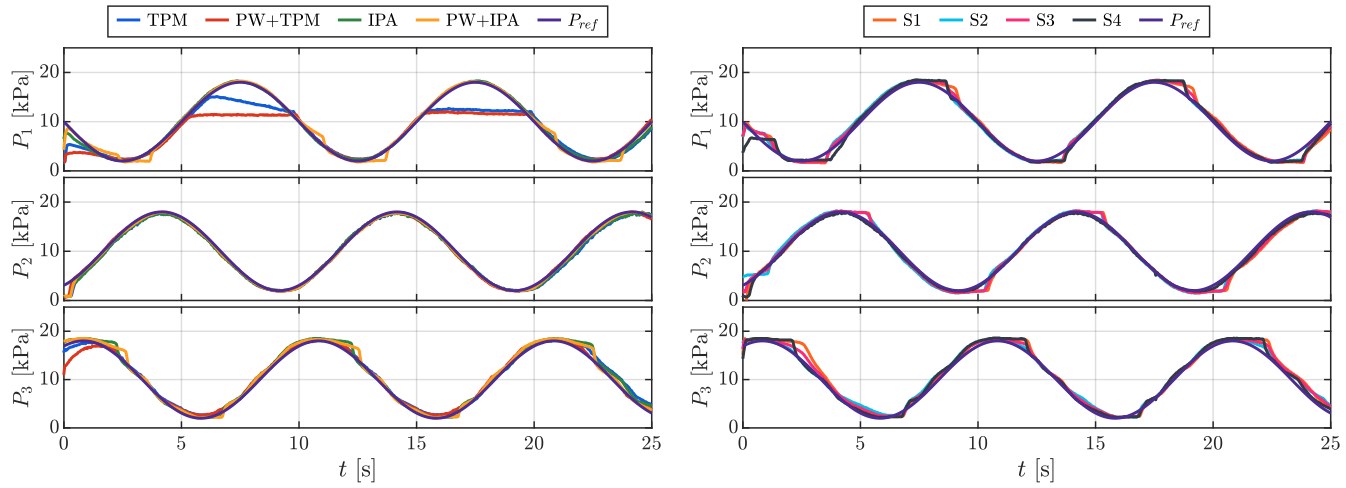

(a) Control group samples cleaned with the standard cleaning procedure

(b) Samples cleaned with our cleaning procedure

Fig. 7: Measured and commanded pressure for two groups of Three-bellow SFAs. (a) Control group SFAs manufactured using the standard cleaning procedure. Control group SFAs are either pre-washed (PW) or not, and are cleaned with either TPM or IPA. Both TPM washed SFAs are not able to reach the commanded pressure in the first bellow, indicating that these bellows are ruptured. (b) Sample (S) SFAs manufactured using our cleaning procedure. Note that, besides the two ruptured bellows (in a), all bellows (in both figures) can be accurately pressure-controlled and the span of the workspace of the SFAs can be compared.

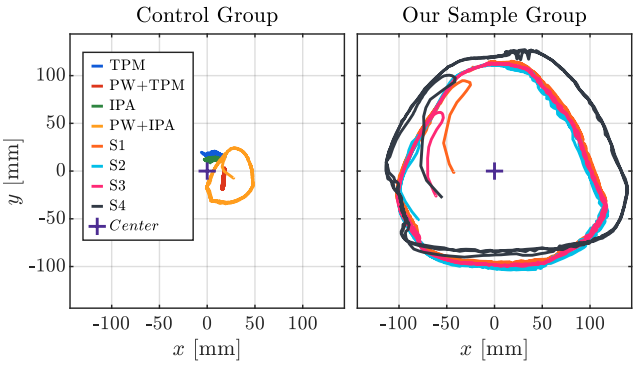

Fig. 8: Planar motion of the SFAs obtained from the control group of SFAs and our sample group using our cleaning procedure. The marked center of each plot is the symmetrical axis of the SFAs. Due to the insufficient cleaning of the control group, the excess cured resin restricts the motion of the SFAs. For identical commanded pressures, our sample group has an significantly larger span of the workspace, showing that our cleaning procedure is better at removing the uncured resin before the post-curing step.

where $\phi_i = (i-1)\pi/3$ is the phase offset of the i-th bellow. In ideal conditions, the resulting motion of the end-effector should be symmetric w.r.t. to the geometric center axis of the SFA (i.e., the backbone curve). Fig. 7 the measured and commanded pressure signals per bellow for both groups of SFAs. Fig. 8 shows the planar motion of the SFAs end-effector obtained using a vision system (Intel Realsense D435).

For the control group, we can observe that for three of the SFAs little to no motion occurs when pressurizing individual bellows. From these SFAs, two have a ruptured bellow, which can be seen from the measured pressure not reaching the commanded pressure. Only one SFA is able to achieve a motion that encircles a region, however, this motion does not encircle the symmetrical axis.

Analyzing the results of our SFAs cleaned with the procedure described in Sec. III-C, we observe that three SFAs show near-identical behavior when pressurizing individual bellows. Additionally, there are no ruptured bellows and the span of the workspace of this set of SFAs is significantly larger than the control group. The behavior is also more symmetric around the symmetry axis than the behavior of the control group.

Remark. *It is observed that sample 4 has a larger span of the workspace compared to the other samples. A reason for this could be that the material undergoes additional curing after the post-curing step when subjected to sunlight, which increases the material's stiffness. Samples 1-3 (S1-3) were made at the same time, while sample 4 (S4) was manufactured a month later, lending credence to the assumed cause of the lower stiffness of S4. In addition, we observed an optical difference between S1-3 and S4. Namely, S4 is noticeably more opaque than set S1-3. Investigating the cause and whether the difference in stiffness and appearance are linked is outside the scope of this work.*

These observations show that, without proper cleaning, the residual resin can introduce significant anisotropic behavior. Comparing our samples to the control group, the span of the workspace is significantly larger, more symmetric, and has less variation w.r.t other samples – indicating that the original geometry is better preserved in the final 3D-printed part.

Additional actuators were also manufactured and cleaned to ensure that the cleaning procedure works regardless of the SFA geometry. All of these actuators showed no signs of excess cured resin. The positive pressure gripper was tested in tandem with the three-bellow SFA and was able to grasp and move objects successfully. The topology-optimized bending actuator was able to bend without issue. Additionally, it was observed during cleaning that due to the large cavities,

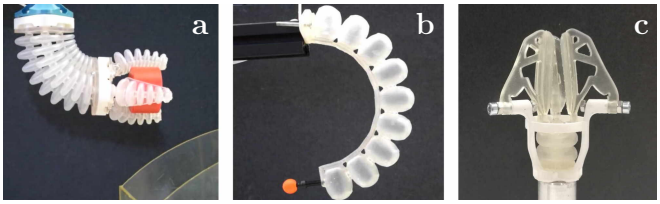

Fig. 9: The additional actuators in their activated state. (a) The positive pressure gripper grasping an object. (b) The topology-optimized bending actuator when bending. (c) The vacuum gripper when closed.

the excess resin could more easily dissolve into the TPM. Finally, the topology-optimized vacuum gripper was able to close completely. An illustrative example of the additional SFAs in their activated state are shown in Fig. 9.

V. Conclusions

In this paper, we presented a method to easily clean SFAs with complex internal geometries. Our results show that the designed pump and subsequently developed cleaning procedures can remove most, if not all, uncured resin from the internal structure of an SLA/DLP printed SFA. The procedure ensures that the desired internal geometries are reflected in the final printed soft actuators. The pump could also be used to clean soluble internal molds to aid in developing SFAs using silicon molding or complex geometries in hard material.

To conclude, our presented cleaning method makes the cleaning of printed structures with complex internal geometries easier and simplifies the process of (re)producing soft (robotic) systems.

References

[1] G. Robinson and J. B. C. Davies, "Continuum robots - a state of the art," in *Proceedings 1999 IEEE International Conference on Robotics and Automation (Cat. No.99CH36288C)*. IEEE, May 1999, vol. 4, pp. 2849–2854.

[2] D. Trivedi, A. Lotfi, and C. D. Rahn, "Geometrically Exact Models for Soft Robotic Manipulators," *IEEE Transactions on Robotics*, vol. 24, no. 4, pp. 773–780, Jul. 2008.

[3] D. Rus and M. T. Tolley, "Design, fabrication and control of soft robots," *Nature*, vol. 521, no. 7553, pp. 467–475, 2015.

[4] H. Abidi, G. Gerboni, M. Brancadoro, J. Fras, A. Diodato, M. Cianchetti, H. Wurdemann, K. Althoefer, and A. Menciassi, "Highly dexterous 2-module soft robot for intra-organ navigation in minimally invasive surgery," *International Journal of Medical Robotics and Computer Assisted Surgery*, vol. 14, no. 1, p. e1875, Feb. 2018.

[5] H. Al-Fahaam, S. Davis, and S. Nefti-Meziani, "Wrist rehabilitation exoskeleton robot based on pneumatic soft actuators," in *2016 International Conference for Students on Applied Engineering (ICSAE)*. IEEE, Oct. 2016, pp. 491–496.

[6] J. Shintake, V. Cacucciolo, D. Floreano, and H. Shea, "Soft Robotic Grippers," *Advanced Materials*, vol. 30, no. 29, p. 1707035, Jul. 2018.

[7] N. El-Atab, R. B. Mishra, F. Al-Modaf, L. Joharji, A. A. Alsharif, H. Alamoudi, M. Diaz, N. Qaiser, and M. M. Hussain, "Soft Actuators for Soft Robotic Applications: A Review," *Advanced Intelligent Systems*, vol. 2, no. 10, p. 2000128, Oct. 2020.

[8] M. S. Xavier, A. J. Fleming, and Y. K. Yong, "Finite Element Modeling of Soft Fluidic Actuators: Overview and Recent Developments," *Advanced Intelligent Systems*, vol. 3, no. 2, p. 2000187, Feb. 2021.

[9] C. Laschi, B. Mazzolai, and M. Cianchetti, "Soft robotics: Technologies and systems pushing the boundaries of robot abilities," *Science Robotics*, vol. 1, no. 1, p. eaah3690, Dec. 2016.

[10] A. D. Marchese, R. K. Katzschmann, and D. Rus, "A Recipe for Soft Fluidic Elastomer Robots," *Soft Robotics*, vol. 2, no. 1, pp. 7–25, 2015.

[11] C. Tawk and G. Alici, "A Review of 3D-Printable Soft Pneumatic Actuators and Sensors: Research Challenges and Opportunities," *Advanced Intelligent Systems*, vol. 3, no. 6, p. 2000223, Jun. 2021.

[12] M. S. Xavier, C. D. Tawk, A. Zolfagharian, J. Pinskier, and A. J. Fleming, "Soft Pneumatic Actuators: A Review of Design, Fabrication, Modeling, Sensing, Control and Applications," *IEEE Access*, vol. 10, pp. 59 442–59 485, Jun. 2022.

[13] W. Hu and G. Alici, "Bioinspired Three-Dimensional-Printed Helical Soft Pneumatic Actuators and Their Characterization," *Soft Robotics*, vol. 7, no. 3, pp. 267–282, Jun. 2020.

[14] B. A. W. Keong and R. Y. C. Hua, "A Novel Fold-Based Design Approach toward Printable Soft Robotics Using Flexible 3D Printing Materials," *Advanced Materials Technologies*, vol. 3, no. 2, p. 1700172, Feb. 2018.

[15] D. K. Patel, A. H. Sakhaei, M. Layani, B. Zhang, Q. Ge, and S. Magdassi, "Highly Stretchable and UV Curable Elastomers for Digital Light Processing Based 3D Printing," *Advanced Materials*, vol. 29, no. 15, p. 1606000, Apr. 2017.

[16] C. J. Thrasher, J. J. Schwartz, and A. J. Boydston, "Modular Elastomer Photoresins for Digital Light Processing Additive Manufacturing," *ACS Applied Materials & Interfaces*, vol. 9, no. 45, pp. 39 708–39 716, Nov. 2017.

[17] B. N. Peele, T. J. Wallin, H. Zhao, and R. F. Shepherd, "3D printing antagonistic systems of artificial muscle using projection stereolithography," *Bioinspiration & Biomimetics*, vol. 10, no. 5, p. 055003, Sep. 2015.

[18] Y.-F. Zhang, C. J.-X. Ng, Z. Chen, W. Zhang, S. Panjwani, K. Kowsari, H. Y. Yang, and Q. Ge, "Miniature Pneumatic Actuators for Soft Robots by High-Resolution Multimaterial 3D Printing," *Advanced Materials Technologies*, vol. 4, no. 10, p. 1900427, Oct. 2019.

[19] T. J. Wallin, J. H. Pikul, S. Bodkhe, B. N. Peele, B. C. Mac Murray, D. Therriault, B. W. McEnerney, R. P. Dillon, E. P. Giannelis, and R. F. Shepherd, "Click chemistry stereolithography for soft robots that self-heal," *Journal of Materials Chemistry B*, vol. 5, no. 31, pp. 6249–6255, Aug. 2017.

[20] K. Yu, A. Xin, H. Du, Y. Li, and Q. Wang, "Additive manufacturing of self-healing elastomers," *NPG Asia Materials*, vol. 11, no. 7, pp. 1–11, Feb. 2019.

[21] A. K. Mishra, T. J. Wallin, W. Pan, P. Xu, K. Wang, E. P. Giannelis, B. Mazzolai, and R. F. Shepherd, "Autonomic perspiration in 3D-printed hydrogel actuators," *Science Robotics*, vol. 5, no. 38, p. eaaz3918, Jan. 2020.

[22] A. Costas, D. E. Davis, Y. Niu, S. Dabiri, J. Garcia, and B. Newell, "Design, Development and Characterization of Linear, Soft Actuators via Additive Manufacturing," *American Society of Mechanical Engineers Digital Collection*, Nov. 2018.

[23] Silisand. Peristaltic pump improved for nema 17 - thingiverse. (Accessed Sep 12-2022). [Online]. Available: https://www.thingiverse.com/thing:1134817

[24] B. Proper, "Peristaltic pump documentation," https://github.com/ReshapeTUe/Peristaltic-Pump-Documentation, 2022.

[25] Formlabs. Using the form wash. (Accessed October 06-2022). [Online]. Available: https://support.formlabs.com/s/article/Using-Form-Wash?language=en_US#form-wash-workflow

[26] B. J. Caasenbrood, F. E. van Beek, H. K. Chu, and I. A. Kuling, "A Desktop-sized Platform for Real-time Control Applications of Pneumatic Soft Robots," in *2022 IEEE 5th International Conference on Soft Robotics (RoboSoft)*. IEEE, Apr. 2022, pp. 217–223.

[27] TU/e. 3d printing facilities. (Accessed October 12-2022). [Online]. Available: https://www.tue.nl/en/education/tue-innovation-space/about/facilities/3d-printing-facilities/

[28] B. Caasenbrood, A. Pogromsky, and H. Nijmeijer, "A Computational Design Framework for Pressure-driven Soft Robots through Nonlinear Topology Optimization," in *2020 3rd IEEE International Conference on Soft Robotics (RoboSoft)*. IEEE, May 2020, pp. 633–638.

[29] B. Caasenbrood, "Sorotoki - a soft robotics toolkit for matlab," https://github.com/BJCaasenbrood/SorotokiCode, 2020.